Study on the Action Mechanism of *Abelmoschus manihot* in Treating Cardiovascular and Cerebrovascular Diseases Based on UPLC-Q-TOF-MS/MS Combined with Network Pharmacology and Molecular Docking

Weixian YANG[1,2], Weiqing ZHANG[2], Xianji LIU[2], Meiqi WEI[1,2], Meihui DUAN[1,2], Chen YAN[1,2]*

1. Guizhou University of Traditional Chinese Medicine, Guiyang 550000, China; 2. Anshun City People's Hospital, Anshun 561000, China

Abstract [**Objectives**] The targets and mechanism of *Abelmoschus manihot* in the treatment of cardiovascular and cerebrovascular diseases were predicted based on UPLC-Q-TOF-MS/MS, network pharmacology and molecular docking techniques. [**Methods**] UPLC-Q-TOF-MS/MS was applied to rapidly analyze chemical components of *A. manihot*. Active components and potential targets of *A. manihot* were retrieved from TCMSP and Swiss Target Prediction database. Cardio-cerebrovascular disease targets were screened using GeneCards database, and Venny 2.1.0 was employed to obtain common targets of *A. manihot* in the treatment of cardiovascular and cerebrovascular diseases. A PPI network was constructed using String platform. The network topology of Cytoscape. 3.10.2 software was used to compute and screen key targets, and GO and KEGG pathway enrichment analysis was carried out in Metascape database to construct a "herb-component-target-pathway-disease" network using Cytoscape. 3.10.2 software. Molecular docking was used to predict the binding properties of active ingredients and targets. [**Results**] The results of UPLC-Q-TOF-MS/MS showed that 56 compounds were identified from *A. manihot*. The results of network pharmacological analysis showed that 54 active ingredients were screened, and 167 common targets of the *A. manihot* and cardiovascular and cerebrovascular diseases were identified, among which the key targets were ALB (albumin), IL6 (interleukin-6), TNF (tumor necrosis factor), AKT1 (serine/threonine protein kinase 1) and GAPDH (glyceraldehyde triphosphate dehydrogenase). KEGG enrichment analysis showed that key signaling pathways include pathways in cancer, lipid and atherosclerosis, PI3K-Akt signaling pathway, Rap1 signaling pathway, proteoglycans in cancer, HIF-1 signaling pathway, cAMP signaling pathway and other signaling pathways. Molecular docking results showed that α-linolenic acid, naringenin, morin, kaempferol, myricetin, quercetin, ethyl caffeate, ellagic acid and atractyloside A might be the key components of *A. manihot* in the treatment of cardiovascular and cerebrovascular diseases. [**Conclusions**] The results suggest that through the combination of UPLC-Q-TOF-MS/MS and network pharmacology and molecular docking methods, it was initially clarified that *A. manihot* can treat cardiovascular and cerebrovascular diseases through multiple components, multiple targets and multiple pathways.

Key words *Abelmoschus manihot*; UPLC-Q-TOF-MS/MS; Network pharmacology; Molecular docking; Cardiovascular and cerebrovascular diseases

DOI: 10.19759/j.cnki.2164-4993.2024.06.018

Cardiovascular and cerebrovascular diseases mainly involve nervous system diseases and circulatory system diseases with heart, brain and blood vessels as target organs, and have the characteristics of complex pathogenesis, high morbidity, disability rate and mortality rate[1-3]. Cardiovascular and cerebrovascular diseases mainly include hypertension, hyperlipidemia, coronary atherosclerosis, thrombosis, angina pectoris and cerebral infarction[4]. The etiology and mechanism of cardiovascular and cerebrovascular diseases are not clear. At present, most of the clinical treatments are drugs aimed at the etiology, including antihypertensive drugs, statins, hypoglycemic drugs, *etc.*, and there are problems such as difficulties in stopping taking drugs, drug resistance and adverse reactions[5]. Chinese herbal medicine regulators have few adverse reactions, and great advantages such as multiple components, multiple sites and multiple targets. Therefore, the research and development of medicinal and edible plants for the treatment of cardiovascular and cerebrovascular diseases has become a hot topic in the field of medicine[6].

Abelmoschus manihot is an annual herbaceous plant of *Abelmoschus*, also known as Caifurong, Yefurong, and Shanyupi. It is known as the "giant panda" of the plant kingdom[7]. It not only has the function of dual-use medicine and food, but also has health efficacy. In the research of modern pharmacodynamics, the chemical components of *A. manihot* are complex, mainly including flavonoids[8], unsaturated fatty acids[9], polysaccharides[10] and trace elements[11], which have many pharmacological effects such as antioxidation, cancer resistance, immunomodulation and prevention of cardiovascular and cerebrovascular diseases[12-13]. Studies have shown that flavonoids and unsaturated fatty acids in *A. manihot* can clear cholesterol in plasma, and have obvious effect of improving hyperlipidemia. Thus, *A. manihot* can be used to treat cardiovascular and cerebrovascular diseases such as hypertension and hyperlipidemia[14-17]. However, the material basis of *A. manihot* for treating cardiovascular and cerebrovascular diseases and its action mechanism are not clear. Therefore, in this study, in order to clarify the active components of *A. manihot* in the treatment of cardiovascular and cerebrovascular diseases and its potential mechanism of action, *A. manihot* was selected as the

Received: August 17, 2024 Accepted: October 9, 2024

Supported by Science and Technology Fund Project of Guizhou Provincial Health Commission (gzwjk2024-241).

Weixian YANG (1998 -), female, master, devoted to research about chemistry and active components of natural medicines.

* Corresponding author.

research object, which was qualitatively identified by UPLC-Q-TOF-MS /MS for its active components, and the active components, targets and mechanism of *A. manihot* in the treatment of cardiovascular and cerebrovascular diseases were predicted by combining network pharmacology and molecular docking.

Materials and Methods

Materials

Instruments: Dionex Ultimate 3000 RSLC (HPG), Thermo Fisher Scientific; Thermo Scientific Q Exactive Focus, Thermo Fisher Scientific; HESI-II, Thermo Fisher Scientific; ACE Ultracore2.5 SuperC18: 100 mm × 2.1 mm.

Reagents: 95% ethanol; methanol (chromatographically pure); acetonitrile (chromatographically pure); formic acid.

Medicinal material: Dried flowers of *A. manihot*.

Methods

Sample treatment and instrument conditions Sample treatment: A 21.1 g of dried *A. manihot* sample was weighed, and then added with 95% ethanol to a level 3 – 5 cm higher than the material and reflux-extracted twice, 3 h each time. After filtration, the filtrates were combined. Next, ethanol was recovered from the filtrate under reduced pressure to obtain a thick paste. Subsequently, 10.1 mg of extract was weighed, and dissolved in 70% methanol water. Finally, the dissolved extract was filtered with 0.22 μm organic microporous membrane to obtain the sample of *A. manihot*.

Chromatographic conditions: ACE Ultracore2.5 SuperC18 column (100 mm × 2.1 mm); acetonitrile (0.1% formic acid)-0.1% formic acid water as mobile phase; gradient elution; volume flow: 0.4 ml/min; injection volume: 2.0 μl; column temperature: 40 ℃.

Mass spectrometry conditions: HESI-II ion source; positive and negative ion mode; ion source voltage: 3.0 kV (+)/2.5 kV (−); capillary heating temperature: 320 ℃; sheath gas flow rate: 35 arb; auxiliary gas flow rate: 10 arb, ion source temperature: 350 ℃; mass spectrometry scanning mode: full MS-ddms2; scanning range: 100 – 1 500 m/z; full MS primary resolution: 70 000, secondary resolution: 17 500.

Data analysis: The data of *A. manihot* were retrieved by Compound discover software. The primary and secondary mass spectrometry data provided by mass spectrometry scanning were analyzed to identify the compounds. The identified chemical components of *A. manihot* were screened and determined.

Collection of components in *A. manihot* and target prediction of active components Through Pubchem database[18] (https://pubchem.ncbi.nlm.nih.gov/), each compound obtained by rapid analysis was searched for the number of Canonical SMILES. The numbers of Canonical SMILES were copied, or the 2D structures were downloadeded and saved in SDF format. The copied Canonical SMILES numbers or 2D structures in SDF format were uploaded to Swiss Target Prediction database[19] (http://swisstargetprediction.ch/), and with the attribute set as "Homo sapiens", Predict targets was clicked to perform prediction and analysis, and compound target information was exported and saved in CSV format. Excel was used to combine chemical targets, and the targets with "probability > 0" were selected in the prediction results. Duplicate data were removed to get the targets of active components. InChIKey of compounds, for which no target was obtained, was uploaded to TCMSP database[20] (https://old.tcmsp-e.com/tcmsp.php), and targets in Related targets were all copied into an excel data table. The data were processed, and those in the target name column were uploaded to Uniplot database[21] (https://www.uniprot.org/) to search for gene names, and the obtained data were downloaded. After normalizing the collected targets to official names, duplicate values were removed, and the results from the two times of prediction were combined.

Collection of targets related to cardiovascular and cerebrovascular diseases and acquisition of herb-disease common targets Genes related to cardiovascular diseases were searched on the platform of GeneCards database[22] (https://www.genecards.org), with " cardio-cerebrovascular disease" as the key word, and targets related to cardiovascular and cerebrovascular diseases with Relevance score ≥ 5 downloaded from GeneCards database were screened. On-line tool Venny 2.1.0 (http://www.liuxiaoyuyuan.cn/) was employed to intersect the targets of *A. manihot* components and the targets related to cardiovascular and cerebrovascular diseases to obtain intersecting targets.

Construction of protein-protein interaction network diagram (PPI) of *A. manihot* and cardiovascular and cerebrovascular diseases The obtained common targets were introduced into protein/gene interaction String online platform[23] (https://cn.string-db.org/) to construct a protein interaction network (PPI). After selecting "Multiple protein", "Homo Sapiens" and Minimum required interaction score ≥ 0.4, the protein interaction results were downloaded in TSV format, and imported into Cytoscape 3.10.2 software for visual analysis. The Network Analyzer plug-in was employed to screen core targets. The degree, betweenness and closeness were used as evaluation indicators for various targets, and the top 10 intersecting targets with values above the averages of the three were selected as potential key targets.

GO enrichment analysis and KEGG pathway analysis In order to explain the processes involved in the treatment of cardiovascular diseases by compounds in *A. manihot*, the files in TSV format stored in String database were processed. After merging the data of node1 and node2, duplicate values were removed, and the data were imported into Metascape database[24] (http://metascape.org/gp/index.html#/main/step1) to perform GO function and KEGG pathway enrichment analysis. Submit was clicked to select *H. sapiens* (166) as the species, and Custom Analysis was chosen for data analysis. Enrichment was clicked to select GO Biological Processes, GO Cellular Components, GO Molecular

Functions, and KEGG Pathway, respectively, for analysis. The online drawing tool of Bioinformatics Online Platform (http://www.bioinformatics.com.cn/) was adopted to visualize GO diagrams and KEGG diagram.

Construction of "*A. manihot*-component-disease-target-pathway" network diagram After establishing the network and type files of *A. manihot*-component-disease-target-pathway, the results were visualized by Cytoscape 3.10.2 software, and an "*A. manihot*-component-cardiovascular and cerebrovascular disease-target-pathway" network diagram was constructed. The Network Analyzer plug-in was employed to screen core active components, and the components with high degree values were selected as key components, which were exported to Excel files for next molecular docking.

Molecular docking simulation verification The key components and key targets screened in "Construction of protein-protein interaction network diagram (PPI) of *A. manihot* and cardio-cerebrovascular disease" 2.4 and "Construction of "*A. manihot*-component-disease-target-pathway" network diagram" were analyzed. Molecular docking was carried out on the obtained components and targets. The 2D or 3D structures of key components were downloaded through Pubchem or TCMSP database, and the structures downloaded from Pubchem database were saved in SDF format. The 2D or 3D structures in SDF format were converted into files in mol2 format through OpenBable software. Autoduck software was employed to add full hydrogens, and after setting as ligands, detecting torsion bonds and setting torsion bonds, and the data were exported as pdbqt. The PDB structures of various targets were downloaded through PDB database, and Pymol software was employed to dehydrate proteins and remove ligands and solvent molecules. Autoduck software was used to add all hydrogens to the structures, which were then set as receptors and exported as pdbqt. Finally, Autoduck software was used for molecular docking, and the docking results were imported into Pymol software for data visualization to obtain a molecular docking action mode diagram.

Results and Analysis

Main chemical components of *A. manihot*

Samples were treated and detected by UPLC-Q-TOF -MS/MS according to above methods, and the chemical components in the ethanol extract of *A. manihot* were qualitatively analyzed. The total ion chromatograms (TLC) in positive and negative ion modes were obtained, as shown in Fig. 1. According to the compound information generated by mass spectrometry combined with secondary fragment ions and relevant references, the chemical components of *A. manihot* were qualitatively analyzed. A total of 56 compounds were identified from *A. manihot*, including 2 alkaloids, 9 phenols and phenolic acids, 12 flavonoids, 4 phenylpropanoids, 3 coumarins and 29 other compounds. Table 1 shows the data of chemical components, molecular formulas, compound names and fragment ion information.

Prediction on targets of active components in *A. manihot*

Through TCMSP and Swiss Target Prediction database, 56 compounds were predicted. Among them, no similar active substances and predicted targets were found in the target prediction results of 13-α-(21)-epoxyeurycomanone and hematoxylin compounds, so 54 active components were obtained. After removing duplicate values of the obtained targets, a total of 603 potential targets were obtained.

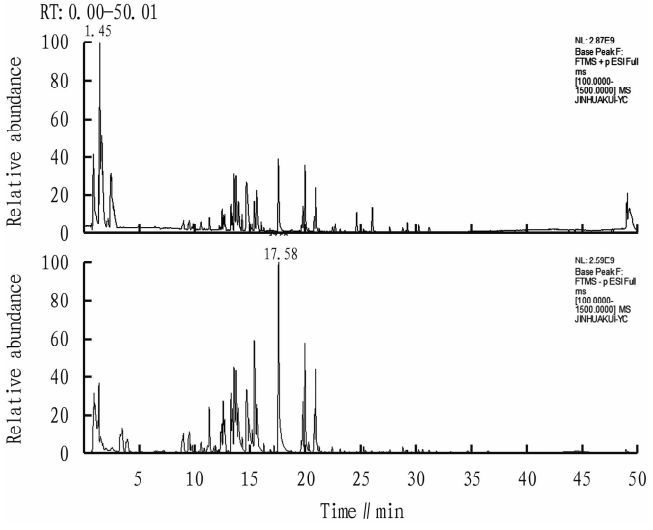

Fig. 1 Total ion chromatograms of *A. manihot*

Screening of active component targets of *A. manihot* and targets of cardiovascular and cerebrovascular diseases

In Genecards database, 2 128 targets related to cardiovascular and cerebrovascular diseases were obtained, and the targets with correlation Score ≥3 were selected as potential targets for treating cardiovascular diseases. After screening, 1 012 related targets were obtained. Next, 603 potential targets of active components in *A. manihot* and 1 012 targets related to cardiovascular and cerebrovascular diseases collected in Genecards database were compared and intersected by Venny 2.1.0, and a Venn diagram was constructed, obtaining 167 common targets, as shown in Fig. 2.

Construction of protein-protein interaction network using common targets of *A. manihot* and cardiovascular and cerebrovascular diseases

A PPI network diagram of common action targets of *A. manihot* in the treatment of cardio-cerebrovascular disease was constructed through the online database of String. The results were visualized with Cytoscape 3.10.2, as shown in Fig. 3. Among the 167 targets, 166 were connected with each other, forming 2 815 kinds of interactions, and the color size of nodes was positively correlated with the degree value. The top 30 common targets were obtained by comprehensive sorting with the values of degree, betweenness and closeness and data sorting and screening with Excel data, as shown in Table 2. These targets were predicted to be key targets of active components in *A. manihot*.

Table 1 Results of composition identification of *A. manihot*

No.	Compound	Molecular formula	Molecular weight	RT//min	Area (Max.)
K1	N6,N6,N6-Trimethyl-L-lysine	$C_9H_{20}N_2O_2$	188.151 92	0.761	3 673 824.002
K2	γ-Aminobutyric acid	$C_4H_9NO_2$	103.063 31	0.894	4 528 942.28
K3	Trigonelline hydrochloride	$C_7H_7NO_2$	137.047 18	0.899	201 543 627
K4	L-Valine	$C_5H_{11}NO_2$	135.089 36	0.900	233 149 483
K5	$C_i$tric acid	$C_6H_8O_7$	192.025 68	0.930	2 659 744.657
K6	Nicotinic acid	$C_6H_5NO_2$	141.042 38	1.351	11 970 607.74
K7	Uridine	$C_9H_{12}N_2O_6$	244.068 54	1.375	8 918 241.329
K8	Adenosine	$C_{10}H_{13}N_5O_4$	267.095 72	1.455	199 962 524.1
K9	Adenine	$C_5H_5N_5$	118.027 55	1.461	90 410 577.11
K10	Guanine	$C_5H_5N_5O$	134.022 36	1.552	53 162 565.19
K11	N-Acetyl-DL-alanine	$C_5H_9NO_3$	131.056 70	1.563	646 088.6343
K12	L-Leucine	$C_6H_{13}NO_2$	131.094 18	1.575	168 435 247.4
K13	Dioxopurine	$C_{10}H_{12}N_4O_6$	284.074 62	1.955	6 662 063.29
K14	Gallic acid	$C_7H_6O_5$	170.020 17	1.969	14 770 765.9
K15	L-Phenylalanine	$C_9H_{11}NO_2$	165.077 56	2.542	18 689 052.46
K16	Protocatechuic acid	$C_7H_6O_4$	154.025 14	3.923	50 126 092.79
K17	5-Hydroxymethylfurfural	$C_6H_6O_3$	126.031 46	4.421	12 943 430.8
K18	L-Tryptophan	$C_{11}H_{12}N_2O_2$	204.089 13	5.22	15 558 500.62
K19	Protocatechualdehyde	$C_7H_6O_3$	138.030 18	6.465	8 658 021.551
K20	Higenamine	$C_{16}H_{17}NO_3$	271.119 86	7.292	6 408 480.905
K21	2-Hydroxy-2-isopropylsuccinic acid	$C_7H_{12}O_5$	176.067 12	7.651	3 689 517.216
K22	1-Caffeoylquinic acid	$C_{16}H_{18}O_9$	354.093 79	9.554	50 674 770.75
K23	Quinicacid	$C_7H_{12}O_6$	192.062 06	9.576	12 535 433.84
K24	$C_o$umarin	$C_9H_6O_2$	164.046 52	9.766	5 823 746.065
K25	Esculetine	$C_9H_6O_4$	178.025 22	9.784	2 948 033.822
K26	$C_a$ffeic acid	$C_9H_8O_4$	180.040 92	10.015	6 994 235.234
K27	$C_r$yptochlorogenic acid	$C_{16}H_{18}O_9$	354.093 91	10.118	3 081 273.097
K28 *	Dihydromyricetin	$C_{15}H_{12}O_8$	320.052 19	11.132	8 763 304.638
K29	Ethyl gallate	$C_9H_{10}O_5$	198.051 56	12.288	2 271 388.928
K30	Isorhamnetin-3-O-neohespeidoside	$C_{28}H_{32}O_{16}$	624.166 87	12.482	50 479 629.64
K31	Rutin	$C_{27}H_{30}O_{16}$	610.151 49	13.303	189 630 827
K32	Isoquercitrin	$C_{21}H_{20}O_{12}$	464.093 83	13.306	7 813 715.375
K33 *	Morin	$C_{15}H_{10}O_7$	302.041 40	13.421	11 526 981.83
K34 *	Ellagic acid	$C_{14}H_6O_8$	302.005 29	13.474	10 735 120.93
K35	Hyperin	$C_{21}H_{20}O_{12}$	464.094 10	14.139	27 943 657.82
K36	Astragalin	$C_{21}H_{20}O_{11}$	448.098 91	14.376	11 657 957.28
K37	p-Hydroxybenzoic acid	$C_7H_6O_3$	138.030 18	14.459	2 889 346.51
K38	Narcissoside	$C_{28}H_{32}O_{16}$	624.166 76	14.467	2 091 211.765
K39	Azelaic acid	$C_9H_{16}O_4$	188.103 50	15.203	7 471 030.698
K40	Ethyl 3,4-dihydroxybenzoate	$C_9H_{10}O_4$	182.056 54	15.415	3 883 068.338
K41 *	Myricetin	$C_{15}H_{10}O_8$	318.036 60	15.79	23 626 843.65
K42	Isomucronulatol 7-O-glucoside	$C_{23}H_{28}O_{10}$	464.167 07	16.482	44 905.594 73
K43	Decanedioic acid	$C_{10}H_{18}O_4$	202.119 25	17.426	950 175.153 9
K44	Norwedelolactone	$C_{15}H_8O_7$	318.036 51	17.58	12 515 644.42
K45 *	Atractyloside A	$C_{21}H_{36}O_{10}$	494.234 66	17.822	2 055 976.102
K46 *	Ethyl caffeinate	$C_{11}H_{12}O_4$	208.072 31	18.074	7 907 647.535
K47 *	Quercetin	$C_{15}H_{10}O_7$	302.041 67	18.117	29 597 133.44
K48 *	Naringenin	$C_{15}H_{12}O_5$	272.067 55	19.101	1 616 008.559
K49 *	Kaempferol	$C_{15}H_{10}O_6$	286.046 72	19.58	4 638 210.937
K50	Kaempferol	$C_{17}H_{34}O_2$	316.260 30	28.243	364 290.169 3
K51 *	α-Linolenic acid	$C_{18}H_{30}O_2$	278.223 55	30.62	3 602 291.597
K52	Methyl vanillate	$C_9H_{10}O_4$	182.056 53	49.126	114 095.24
K53	p-Hydroxy-cinnamic acid	$C_9H_8O_3$	164.045 90	49.384	73 881.591 22
K54	Isoscopoletin	$C_{10}H_8O_4$	192.041 36	49.807	161 671.659 1
K55	13-α-(21)-Epoxyeurycomanone	$C_{20}H_{24}O_{10}$	402.150 98	10.902	17 906 384.32
K56	Hematoxylin	$C_{16}H_{14}O_6$	302.077 96	19.497	35 273.789 85

Those marked with * are key components.

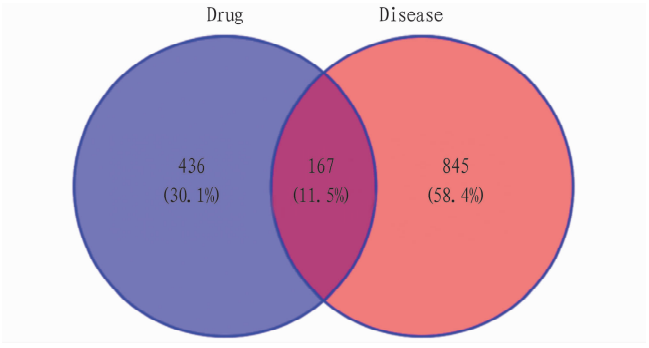

Fig. 2 Common targets of *A. manihot* and cardio-cerebrovascular disease

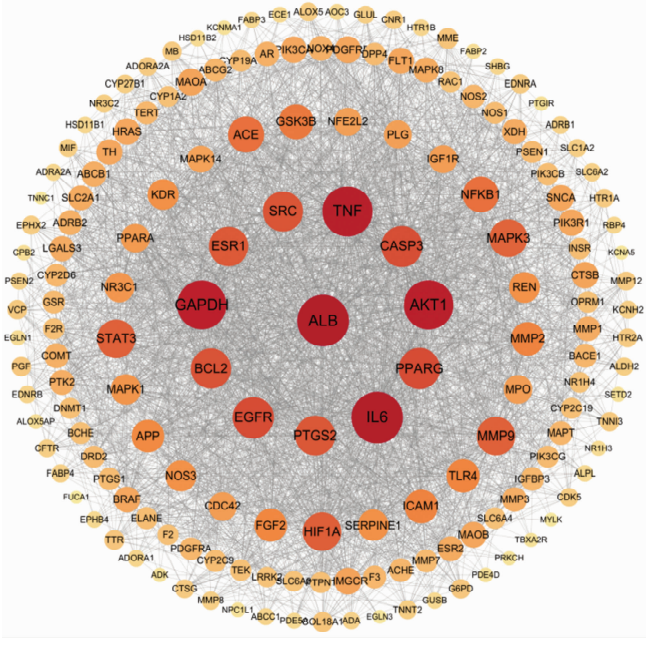

Fig. 3 PPI network for intersecting targets of active components and cardiovascular and cerebrovascular diseases

GO function annotation and KEGG pathway enrichment analysis

In order to explain the processes involved in the treatment of cardiovascular and cerebrovascular diseases by compounds in *A. manihot*, the files in TSV format stored in String database were processed. The data of node1 and node2 were merged to remove duplicate values, and 166 gene targets were obtained. GO and KEGG analysis were carried out using Metascape database. Screening was carried out according to the condition of P Value Cutoff = 0.01, from aspects of biological process (BP), cellular component (CC) and molecular function (MF), and 1 946 BP items, 121 CC items and 214 MF items were obtained respectively. After sorting the LogP values in ascending order, the top 10 items were analyzed, respectively. The results are shown in Fig. 4.

GO analysis showed that biological process items mainly included circulatory system process, response to inorganic substance, response to hormone, cellular response to nitrogen compound, cellular response to organic nitrogen compound, blood circulation, positive regulation of phosphorous metabolic process, positive regulation of phosphate metabolism, reaction to peptide, and positive regulation of cell migration. In terms of cellular component, the targets were mainly involved in membrane raft, membrane microdomain, caveola, cell body, axon, vesicle lumen, plasma membrane raft, neuronal cell body, cytoplasmic vesicle lumen, and dendrite. In terms of molecular function, they were mainly involved in oxidoreductase activity, endopeptidase activity, phosphotransferase activity-alcohol group as receptor, protein kinase activity, heme binding, kinase activity, tetrapyrrole binding, phosphatase binding, kinase binding, and nuclear receptor activity.

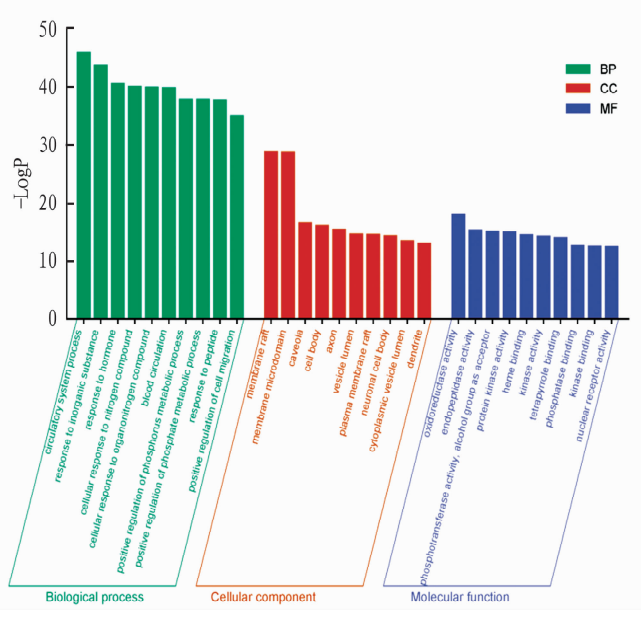

Fig. 4 GO enrichment analysis of potential cardio-cerebrovascular disease targets

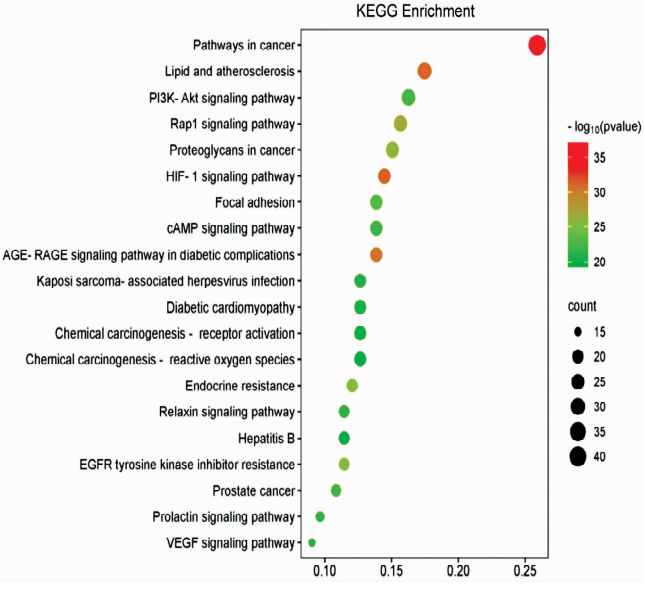

Fig. 5 KEGG pathway enrichment analysis for potential targets of *A. manihot* in treating cardiovascular and cerebrovascular

Table 2 Key targets of the *A. manihot* and their topological features

Name	Closeness	Degree	Betweenness
ALB	0.778 3	118	0.065 4
IL6	0.774 6	117	0.052 6
TNF	0.760 4	113	0.050 1
AKT1	0.750 0	111	0.053 1
GAPDH	0.750 0	110	0.055 2
PPARG	0.679 0	87	0.029 6
EGFR	0.676 2	87	0.027 8
CASP3	0.673 5	86	0.015 2
BCL2	0.668 0	84	0.013 6
SRC	0.662 7	83	0.042 0
PTGS2	0.660 0	82	0.023 9
ESR1	0.660 0	81	0.017 7
HIF1A	0.652 2	79	0.017 2
MMP9	0.649 6	78	0.012 0
STAT3	0.649 6	78	0.009 2
MAPK3	0.649 6	77	0.011 4
ACE	0.634 6	71	0.024 2
NFKB1	0.632 2	71	0.006 1
GSK3B	0.620 3	67	0.011 1
MMP2	0.613 4	63	0.005 9
ICAM1	0.613 4	63	0.005 4
TLR4	0.608 9	62	0.005 8
FGF2	0.611 1	61	0.006 8
APP	0.604 4	60	0.012 7
SERPINE1	0.597 8	56	0.006 7
KDR	0.597 8	56	0.006 0
NOS3	0.595 7	55	0.011 9
REN	0.597 8	55	0.009 7
MAPK1	0.591 4	53	0.005 1

The results of KEGG pathway enrichment showed that 194 pathways were involved, and the bubble diagram of the top 20 KEGG pathways was drawn using the LogP values, as shown in Fig. 5. The results showed that the active components of *A. manihot* for treating cardiovascular and cerebrovascular diseases were mainly distributed in following pathways: pathways in cancer, lipid and atherosclerosis, PI3K-Akt signaling pathway, Rap1 signaling pathway, proteoglycan in cancer, HIF-1 signaling pathway, cAMP signaling pathway, AGE-RAGE signaling pathway in diabetic complications, Kaposi sarcoma-associated herpesvirus infection, diabetic cardiomyopathy, chemical carcinogenesis-receptor activation, chemical carcinogenesis-reactive oxygen species, endocrine resistance, EGFR tyrosine kinase inhibitor resistance, and focal adhesion. These pathways are closely related to the treatment of cardiovascular and cerebrovascular diseases.

Construction of *A. manihot*-component-target-disease-pathway network diagram

The 20 KEGG pathways, 167 interacting potential targets and 54 active components in the above enrichment analysis were jointly analyzed, and an "*A. manihot* -component-target-disease-pathway network diagram" was drawn by Cytoscape 3.10.2 software, as shown in Fig. 6. Topology analysis was carried out using the function "Network Analyzer". Taking degree centrality (DC), betweenness centrality (BC) and closeness centrality (CC) as evaluation indexes, the top 10 active components in terms of degree value were obtained as key active components: K51 (α-linolenic acid), K48 (naringin), K33 (morin), K49 (kaempferol), K41 (myricetin), K47 (quercetin), K46 (ethyl caffeate), K28 (dihydromyricetin), K34 (ellagic acid), and K45 (atractyloside A), as shown in Table 3.

Table 3 Key active components and their topological features

Active components	Degree	Betweennes	Closeness
K51	41	0.130 327 39	0.423 817 863
K48	38	0.062 040 58	0.419 410 745
K33	37	0.034 192 972	0.417 962 003
K49	36	0.029 717 253	0.416 523 236
K41	36	0.029 701 809	0.416 523 236
K47	36	0.028 999 552	0.416 523 236
K46	31	0.052 169 792	0.408 094 435
K28	31	0.044 588 426	0.409 475 465
K34	27	0.023 708 493	0.404 006 678
K45	26	0.036 136 371	0.402 662 23

Molecular docking verification of main active components and targets

Molecular docking was performed on the top 10 key active components (α-linolenic acid, naringin, morin, kaempferol, ethyl 3,4-dihydroxybenzoate, quercetin, ethyl caffeate, dihydromyricetin, ellagic acid and norwedelolactone) and the top five key targets in PPI network: ALB (albumin), IL-6 (interleukin-6), TNF (tumor necrosis factor), AKT1 (serine/threonine protein kinase 1) and GAPDH (glyceraldehyde3-phosphatedehydrogenase). The results of binding energy are shown in Table 4. The binding affinity between protein and ligand was evaluated by docking binding energy (the greater the absolute value of docking score, the stronger the binding affinity). It is generally believed that a binding energy $\leqslant -4.25$ kcal/mol indicates that there is a certain binding activity between the active ingredient and the target; a binding energy $\leqslant -5.0$ kcal/mol indicates that they have good binding activity; and a binding energy $\leqslant -7.0$ kcal/mol indicates that they have strong binding activity[25]. There were six groups with a binding energy less than -7.0 kcal/mol, and the binding energy of all key components and key targets was less than -4.25 kcal/mol, indicating that there was certain binding activity between active components and targets, and both key components and key targets could spontaneously bind, thus playing a role in treating cardiovascular disease. The docking results were well visualized in Pymol software, as shown in Fig. 7.

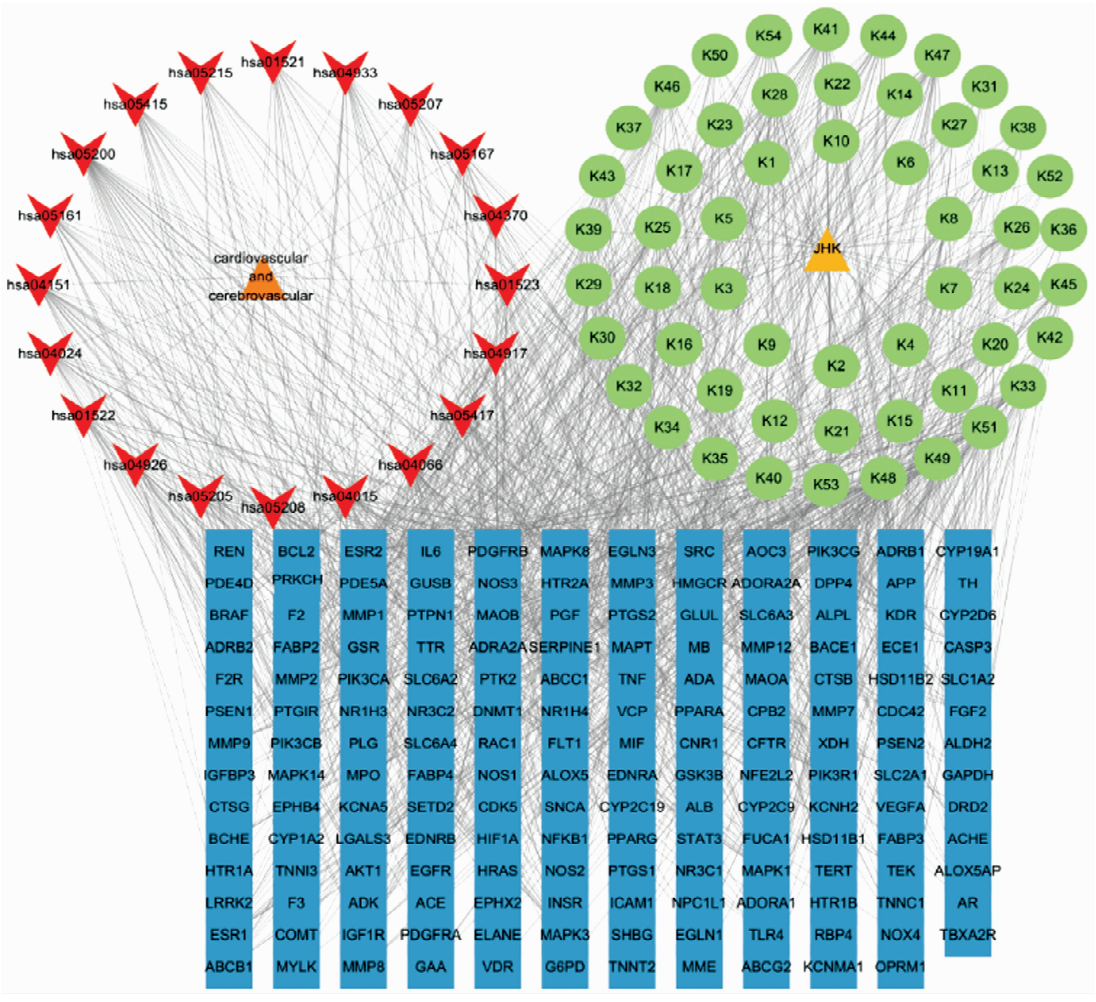

Blue represents targets; red represents pathways; orange represents the disease; yellow represents the herb; and green represents the active components.

Fig. 6 ***A. manihot*-component-disease-target-pathway network**

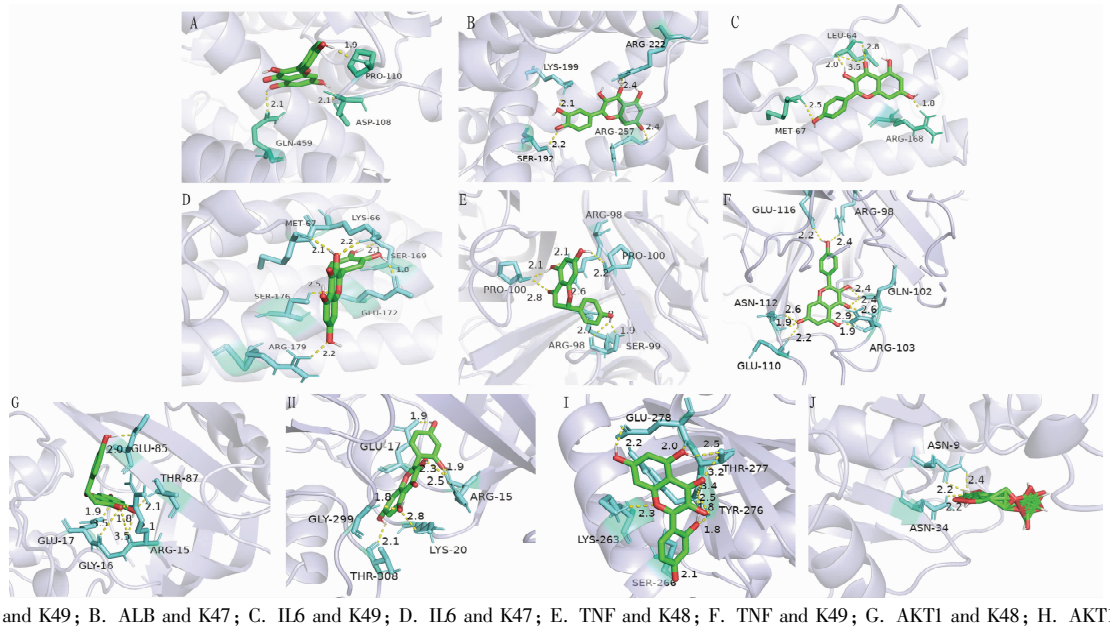

A. ALB and K49; B. ALB and K47; C. IL6 and K49; D. IL6 and K47; E. TNF and K48; F. TNF and K49; G. AKT1 and K48; H. AKT1 and K33; I. GAPDH and K33; J. GAPDH and K45.

Fig. 7 Results of the docking of key targets and key components

Table 4 Molecular docking data of key components and key targets (Kcal/mol)

No.	Compound	ALB	IL6(1alu)	TNF	AKT1(6hhg)	GAPDH(6m61)
K51	α-Linolenic acid	-5.20	-5.44	-5.81	-6.83	-5.72
K48	Naringin	-5.43	-5.94	-7.25	-7.40	-5.31
K33	Morin	-5.15	-5.66	-6.36	-7.40	-5.89
K49	Kaempferol	-6.35	-5.98	-6.81	-7.29	-5.84
K41	Myricetin	-5.64	-5.19	-6.60	-7.32	-5.27
K47	Quercetin	-6.56	-5.98	-6.28	-6.93	-5.80
K46	Ethyl caffeate	-5.52	-5.11	-5.98	-5.93	-4.75
K28	Dihydromyricetin	-5.32	-5.71	-6.16	-7.20	-5.52
K34	Ellagic acid	-4.70	-4.87	-6.71	-5.46	-4.73
K45	Norwedelolactone	-5.03	-4.59	-6.24	-5.66	-5.90

Conclusions and Discussion

In this study, 56 chemical components of *A. manihot* were obtained by UPLC-Q-TOF-MS/MS, and 54 active components were obtained by TCMSP and Swiss Target Prediction database. Then, 167 common targets were obtained after the intersection of active components and cardiovascular and cerebrovascular diseases, and the key targets identified through protein interaction screening for the anti-cardiovascular and cerebrovascular diseases effect of *A. manihot* were ALB (albumin), IL6 (interleukin-6), TNF (tumor necrosis factor), AKT1 (serine/threonine protein kinase 1), and GAPDH (glyceraldehyde3-phosphatedehydrogenase). The "*A. manihot*-component-disease-target-pathway" network diagram intuitively showed that many effective components could play an anti-inflammatory role through multiple targets and pathways. The molecular docking results of active components and key targets suggested that α-linolenic acid, naringin, morin, kaempferol, ethyl 3,4-dihydroxybenzoate, quercetin, ethyl caffeate, dihydromyricetin, ellagic acid and norwedelolactone all had certain binding capacity with key targets, and might be the main active components of *A. manihot* for treating cardiovascular and cerebrovascular diseases, mainly flavonoids and unsaturated fatty acids.

It is reported that the main mechanisms of flavonoids in treating cardiovascular and cerebrovascular diseases are regulating anti-inflammatory factors[26], regulating blood lipid and relaxing blood vessels[27]. The action mechanism of ALB in the occurrence and development of cerebral infarction may be that it inhibits the expression of vascular cell adhesion molecule-1 and increases the clearance of oxygen free radicals, thus reducing inflammatory reaction and endothelial cell apoptosis, or ALB may inhibit the activation and aggregation of platelets by promoting the expression of prostacyclin and inhibiting the activity of thromboxane synthase[28]. Studies have shown that microglia and astrocytes can be over-activated in the pathological process of cerebral ischemia, and a large number of inflammatory factors such as TNF-α, IL-1 and IL-6 can be released. TNF-α as the initial cytokine can induce the further release of IL-1β, which can cause severe inflammatory reaction in brain tissue. The aggravation of inflammation will damage the blood-brain barrier, cause brain edema and cognitive impairment and even lead to death[29-31].

GO analysis showed that *A. manihot* could regulate cardiovascular and cerebrovascular diseases by influencing the activities of oxidoreductase, endopeptidase, heme binding and tetrapyrrole binding. The results of KEGG pathway enrichment showed that the active components of *A. manihot* were mainly distributed in pathways in cancer, HIF-1 signaling pathway, lipid and atherosclerosis, AGE-RAGE signaling pathway in diabetic complications, Rap1 signaling pathway, proteoglycan in cancer, and EGFR tyrosine kinase inhibitor resistance. These pathways are closely related to the treatment of cardiovascular and cerebrovascular diseases.

To sum up, the chemical components were identified by UPLC-Q-TOF-MS/MS. Combined with the network pharmacology method, core targets and action pathways of *A. manihot* in the treatment of cardiovascular and cerebrovascular diseases were predicted, and the core components of *A. manihot* were basically clarified through molecular docking verification. *A. manihot* might act on targets such as ALB, IL-6, TNF, AKT1 and GAPDH, and play a therapeutic role in cardiovascular and cerebrovascular diseases through pathways in cancer, lipid and atherosclerosis, HIF-1 signaling pathway, AGE-RAGE signaling pathway in diabetic complications, Rap1 signaling pathway, and proteoglycan in cancer. Among them, pathways in cancer, lipid and atherosclerosis and HIF-1 signaling pathway might be important regulatory pathways. This study provides a theoretical basis for further experimental research, action mechanism and clinical application of *A. manihot* in treating cardiovascular and cerebrovascular diseases.

References

[1] ZHAO D, LIU J, WANG M, *et al*. Epidemiology of cardiovascular disease in China: Current features and implications[J]. Nature reviews. Cardiology, 2019, 16(4): 203-212.

[2] The Writing Committee of China Cardiovascular Health and Disease Report. Report on cardiovascular health and diseases burden in China: An updated summary of 2020 [J]. Chinese Circulation Journal, 2021, 36(6): 521-545. (in Chinese).

[3] WANG YJ, LI ZX, GU HQ, *et al*. China stroke report 2019 (Chinese version)[J]. Chinese Journal of Stroke, 2020, 15(10): 1037-1043. (in Chinese).

[4] CHEN WW, SUI H, MA LY. Prevalence and prevention progress of cardiovascular and cerebrovascular diseases in China[J]. Prevention and Treatment of Cardio-Cerebral-Vascular Disease, 2016, 16(2): 79-83. (in Chinese).

[5] YANG X, ZHU JP, GUO XX, *et al*. Treatment of cardio-cerebrovascular diseases with Banxia Baizhu Tianmatang: A Review[J]. Chinese Journal of Experimental Traditional Medical Formulae, 2024(16): 1-12. (in Chinese).

[6] XIAO H, GUO YL. Research progress of single-flavored traditional

Chinese medicine regulating intestinal flora against cerebrovascular diseases[J]. Systems Medical, 2023, 8(15): 191 - 194. (in Chinese).
[7] ZHANG YQ, WANG ZW, YE WF. Present situation of application and development of *Aurea helianthus* food[J]. Journal of Datong Vocational College, 2022, 38(3): 76 - 78. (in Chinese).
[8] GUO JL, CHEN Y, XIE ST, *et al.* Research progress of flavonoid hyperoside in *Abelmoschus manihot*[J]. China Food Safety Magazine, 2023(23): 174 - 176. (in Chinese).
[9] LI J, LI PF, LU XD, *et al.* Composition and oxidative stability of fatty acids in oil of *Hibiscus manihot* L. seeds[J]. Fujian Journal of Agricultural Sciences, 2018, 33(7): 755 - 759. (in Chinese).
[10] QIAO XB, XU Y, JIA J. Research progress on active ingredients of *Aurea helianthustems*[J]. Farm Products Processing, 2022(20): 83 - 86. (in Chinese).
[11] GUO XH, BEI ZY. Determination of trace elements in *Aurea helianthus* by microwave digestion-flame atomic absorption spectrometric[J]. China Modern Medcine, 2014, 21(13): 9 - 10. (in Chinese).
[12] JIA J, CHEN P, WANG TT, *et al.* Advances in the extraction and purification of flavonoids from *Hibiscus manihot*[J]. China Fruit & Vegetable, 2024, 44(1): 42 - 46. (in Chinese).
[13] LI J, WANG YF, RONG JD, *et al.* Nutritional value and antioxidant activity of *Abelmoschus manihot* [J]. Chinese Journal of Tropical Crops, 2019, 40(7): 1354 - 1358. (in Chinese).
[14] WU ZP. Effects of unsaturated fatty acids from *Abelmoschus manihot* seeds on blood lipid and liver function in experimental hyperlipidemia rats[J]. Chinese Traditional Patent Medicine, 2011, 33(7): 1245 - 1247. (in Chinese).
[15] LI Y, YANG XS, HE JG. Effect of *Abelmoschus manihot* flavonoids on blood lipid levels of hyperlipidemic rats[J]. Food Science, 2012, 33(1): 248 - 251. (in Chinese).
[16] ZHANG YQ, WANG ZW, YE WF. Research progress of *Aurea helianthus* in the treatment of hyperlipidemia[J]. Journal of Datong Vocational College, 2022, 38(5): 58 - 61. (in Chinese).
[17] XIAO R. Application of hyperoside and therapeutic drug for cerebral ischemia-reperfusion injury: 202111419154. 0[P]. 2022 - 01 - 21. (in Chinese).
[18] KIM S, CHEN J, CHENG T, *et al.* PubChem in 2021: New data content and improved web interfaces[J]. Nucleic Acids Res., 2021, 49(D1): D1388 - D1395.
[19] GFELLER D, MICHIELIN O, ZOETE V. Shaping the interaction landscape of bioactive molecules[J]. Bioinformatics, 2013, 29(23): 3073 - 3079.
[20] RU J, LI P, WANG J, *et al.* TCMSP: A database of systems pharmacology for drug discovery from herbal medicines[J]. J Cheminform., 2014, 6: 13.
[21] UniProt Consortium. UniProt: The universal protein knowledgebase in 2023[J]. Nucleic Acids Res. 2023, 51(D1): D523 - D531.
[22] RAPPAPORT N, TWIK M, PLASCHKES I, *et al.* MalaCards: An amalgamated human disease compendium with diverse clinical and genetic annotation and structured search[J]. Nucleic Acids Res., 2017, 45(D1): D877 - D887.
[23] SZKLARCZYK D, KIRSCH R, KOUTROULI M, *et al.* The STRING database in 2023: Protein-protein association networks and functional enrichment analyses for any sequenced genome of interest[J]. Nucleic Acids Res., 2023, 51(D1): D638 - D646.
[24] ZHOU Y, ZHOU B, PACHE L, *et al.* Metascape provides a biologist-oriented resource for the analysis of systems-level datasets[J]. Nat Commun, 2019, 10(1): 1523.
[25] GAILLARD T. Evaluation of AutoDock and AutoDock Vina on the CASF-2013 benchmark[J]. Journal of Chemical Information and Modeling, 2018, 58(8): 1697 - 1706.
[26] XU D, TAO YM, SONG D, *et al.* Effects of flavone of *Galium verum* L. on atherosclerosis in rabbits based on TLR/NF-κB pathway[J]. Chinese Journal of Integrative Medicine on Cardio-/Cerebrovascuiar Disease, 2022, 20(14): 2540 - 2544. (in Chinese).
[27] SHI JH, WANG XJ, CHENG RQ, *et al.* Research progress on the mechanism of flavonoids in the treatment of cardiovascular and cerebrovascular diseases and its new delivery system[J]. Journal of Inner Mongolia Medical University, 2024, 46(1): 84 - 90. (in Chinese).
[28] LAI XY, YOU ZJ, DENG XL. Analysis of the relationship between fibrinogen/albumin ratio and neurological deficit and prognosis in patients with atherosclerotic cerebral infarction[J]. Neural Injury and Functional Reconstruction, 2024, 19(6): 369 - 372. (in Chinese).
[29] JIANG CC, SHI L, ZHAO XY, *et al.* Mechanism of total flavonoids of *Rhododendra simsii* in alleviating ischemic brain injury [J]. China Journal of Chinese Materia Medica, 2023, 48(2): 455 - 464. (in Chinese).
[30] SHIM R, WONG CHY. Ischemia, immunosuppression and infection-tackling the predicaments of post-stroke complications[J]. International journal of molecular sciences, 2016, 17(1): 64.
[31] LIU M, XU Z, WANG L, *et al.* Cottonseed oil alleviates ischemic stroke injury by inhibiting the inflammatory activation of microglia and astrocyte [J]. Journal of neuroinflammation, 2020, 17: 1 - 15.

Editor: Yingzhi GUANG Proofreader: Xinxiu ZHU

(Continued from page 82)

References

[1] SUNG H, FERLAY J, SIEGEL RL, *et al.* Global cancer statistics 2020: GLOBOCAN estimates of incidence and mortality worldwide for 36 cancers in 185 countries[J]. CA Cancer J Clin., 2021, 71(3): 209 - 249.
[2] QI J, LI M, WANG L, *et al.* National and subnational trends in cancer burden in China, 2005 - 20: an analysis of national mortality surveillance data[J]. Lancet Public Health, 2023, 8(12): e943 - e955.
[3] ROXBURGH P, EVANS TR. Systemic therapy of hepatocellular carcinoma: Are we making progress[J]. Adv Ther., 2008, 25(11): 1089 - 1104.
[4] Chinese Pharmacopoeia Commission. Chinese pharmacopoeia[M]. Beijing: China Medical Science Press, 2015: 83 - 84. (in Chinese).
[5] YAN LG, HUANG JH, LU Y, *et al.* Research progress of hirudin in anticoagulation and anti-tumor metastasis[J]. Traditional Chinese Drug Research and Clinical Pharmacology, 2010, 21(6): 667 - 670. (in Chinese).
[6] LIU X, GAO MF, KONG Y. Bioactive constituents and pharmacological effects of leech[J]. Chinese Journal of Pharmaceutical Biotechnology, 2017, 24(1): 76 - 80. (in Chinese).
[7] JUNREN C, XIAOFANG X, HUIQIONG Z, *et al.* Pharmacological activities and mechanisms of hirudin and its derivatives: A review[J]. Front Pharmacol., 2021, 12: 660 - 757.
[8] CHENG XM, ZHANG M, WANG JH, *et al.* Research progress of hirudin[J]. Journal of Jilin Medical College, 2021, 42(2): 135 - 137. (in Chinese).
[9] ZHANG J, ZHANG Y. Application of leech in tumor diseases[J]. Hunan Journal of Traditional Chinese Medicine, 2006, 22(4): 69. (in Chinese).
[10] HU L, IBRAHIM S, LIU C, *et al.* Thrombin induces tumor cell cycle activation and spontaneous growth by down-regulation of p27Kip1, in association with the up-regulation of Skp2 and MiR-222[J]. Cancer Res. 2009, 69(8): 3374 - 3381.
[11] ZHANG B, WANG XM, REN QH, *et al.* Effects of compound hirudin on the expression of p53, Ki-67 and VECF in transplanted tumor tissues of mice[J]. Shandong Medical Journal, 2008, 48(43): 26. (in Chinese).

Editor: Yingzhi GUANG Proofreader: Xinxiu ZHU